The reaction between aluminium and dimethyl ether Comparative study of density functional theory and EPR results

FARADAY

The reaction between aluminium and dimethyl ether

Comparative study of density functional theory and EPR results

Torbjörn Fängström,[a] Adam Kirrander,[a] Leif A. Eriksson[a,b]* and Sten Lunell[a]

[a] *Department of Quantum Chemistry, Uppsala University, Box 518, S-751 20 Uppsala, Sweden*

[b] *Department of Physics, Stockholm University, Box 6730, S-113 85 Stockholm, Sweden*

Stationary points on the surface describing the reaction between aluminium and dimethyl ether (DME) have been located using density functional theory at the B3LYP level with a 6-31G(d,p) basis set. Hyperfine coupling constants (HFCC) of Al and the proton attached to it, as well as total energies, were computed at all stable structures using the B3LYP and BP86 functionals and the 6-311 + G(2df,p) basis. Compared to earlier theoretical studies, additional stable conformers have been identified. An initial addition complex is formed between Al and CH_3OCH_3, located 4–9 kcal mol^{-1} below the free reactants in energy, depending on computational method. A first transition state connects the addition complex with a structure in which one hydrogen has migrated to the Al atom, whereafter a more stable C—H insertion structure is reached through a second transition state. A second reaction path leading to two C—O insertion products, starting from the addition complex, is also described. The most stable products are the *cis* and *trans* conformers of an open chain C—O insertion product which lie 58–65 kcal mol^{-1} below the reactants in energy. Among the C—H insertion products the most stable ones are cyclic *cis* and *trans* structures, which are found to lie 9–10 kcal mol^{-1} below the reactants.

Several experimental investigations of reactions between aluminium atoms and small organic molecules such as ethylene,[1–3] acetylene,[2,4] buta-1,3-diene,[5] propyne,[6] benzene[7] and several ethers[8–10] have been presented during the last 25 years. Also a number of theoretical works on the above-mentioned reactions and/or its products have been performed, *cf.* ref. 11–16.

Recently, Chenier *et al.* studied the reaction of ground-state aluminium atoms with dimethyl ether on inert hydrocarbon surfaces at 77 K, using EPR techniques.[10] From the Al hyperfine coupling constants (HFCC) obtained, they suggest an assignment to four possible products (I–IV): (i) a mono-ligand complex between Al and a DME molecule, with Al binding to the DME oxygen atom; (ii) a di-ligand complex between one Al atom and two DME, similar to (i); (iii) a reaction product formed by the insertion of an Al atom into a C—O bond of the ether; and finally (iv) a second insertion product resulting from Al insertion into a C—H bond. Chenier *et al.* reported one proton HFCC for only one of the suggested products, for the other three products no proton HFCC were resolved. The most and second most intense sextets observed in the EPR spectra were tentatively assigned to the C—O insertion product and the mono-ligand complex, respectively.

A subsequent theoretical investigation of the reaction, using *ab initio* calculations at the Hartree–Fock and MP2 levels has been reported by Sakai.[11] In this study a mono-ligand complex, a complex where one of the hydrogens has migrated to the Al atom, an open chain C—O insertion product and one cyclic and one open chain C—H insertion product were found. However, to our knowledge no comparison between the experimental HFCCs and theoretical data has so far been carried out, in order to reveal the detailed nature of the observed reaction products.

The aim of the present work is to compare calculated isotropic HFCCs for the possible products of the described reaction with experimental EPR data, to locate stationary points on the potential-energy surface (PES) and to extend the theoretical framework by including density functional theory (DFT).

Methods

Geometries

In all calculations the program systems Gaussian 92[17] and Gaussian 94[18] were used. The functional used in the optimizations, referred to as B3LYP, is based on Becke's three-parameter adiabatic connection method (ACM) approach,[19] and consists of a combination of Slater,[20] Hartree–Fock[21] and Becke[22] exchange, and the Vosko, Wilk and Nusair (VWN) local[23] and Lee, Yang and Parr (LYP)[24] non-local correlation functional. The split valence 6-31G(d,p)[25,26] basis set was used in all optimizations.

Energies

To obtain more reliable total energies at the different stationary points on the PES, single point calculations were carried out using the 6-311 + G(2df,p)[27–31] basis set, using the B3LYP and the BP86 functionals. The latter functional is constructed from the non-local exchange functional by Becke[22] together with Perdew's gradient corrected correlation functional.[32]

Isotropic hyperfine coupling constants

Magnetic interactions between the nuclear spin ($\vec{I}$) and the electronic magnetic moments, caused by the electron spin ($\vec{S}$), give rise to hyperfine splittings in molecular EPR spectra. The splittings can be divided into an isotropic and an anisotropic part, where the isotropic part is given by a contact interaction term (Fermi contact)[33,34] in the spin Hamiltonian:

$$\hat{H}^{(1)}_{\text{spin}} = A_N^{(\text{iso})}(\hat{\boldsymbol{I}} \cdot \hat{\boldsymbol{S}}) \tag{1}$$

For a particular nucleus N (assuming a doublet radical) $A_N^{(\text{iso})}$ is:

$$A_N^{(\text{iso})} = \frac{8\pi}{3} g\beta g_N \beta_N \rho^{(\alpha-\beta)}(\boldsymbol{r}_N) \tag{2}$$

where $\rho^{(\alpha-\beta)}(\boldsymbol{r}_N)$ is the spin density at the position of the nucleus, β is the Bohr magneton, β_N is the nuclear magneton and g and g_N are the electronic and nuclear g values, respectively.

The isotropic hyperfine coupling constants (HFCCs) are thus related to the spin density at a particular nucleus, which can be acquired from a calculated wavefunction. Hence, comparisons with measured hyperfine splittings give a good indication of the quality of the calculated wavefunction and the ability of the method in question to accurately describe the system under study. Here, were report HFCCs for the Al atom and the hydrogens, at those points on the potential-energy surface believed to represent possible reaction products. Results are presented from the B3LYP and BP86 calculations, using the 6-311 + G(2df,p) basis set.

Results

Potential-energy surface

The PES turned out to be extremely corrugated and a large number of stationary points were found at the computational level presently employed.

Altogether 23 points of interest have been located on the potential-energy surface: one addition complex (AC), one di-ligand complex, eleven transition states, eight C—H insertion products and two C—O insertion products. Table 1 lists the relative energies of the B3LYP/6-31G(d,p) optimized structures, obtained from single point calculations using the B3LYP and BP86 functionals in conjunction with the larger 6-311 + G(2df,p) basis. Fig. 1–4 depict the geometries of the optimized stationary points.

The products and transition states were verified to be true energy minima and saddle points of first order, respectively, in frequency calculations performed at the B3LYP/6-31G(d,p) level.

To verify the relevance of the transition states found, intrinsic reaction coordinate IRC[35,36] calculations were performed starting from the different transition states.

Addition complexes. In both complexes the structures of the DME fragments differ only slightly from the geometry of the free DME molecule (*cf.* Fig. 1 and 2). The weak interaction between the constituents can also be seen in the rather large Al—DME bond distances, around 2.2 Å for the mono-ligand and 2.4 Å for the di-ligand complexes. In the addition complex the aluminium, oxygen and carbon atoms are all in one plane. The di-ligand complex is non-planar, close to C_{2v} symmetry, with an O—Al—O angle of 87° (*cf.* Fig. 1).

Table 1 Energies in kcal mol^{-1} given relative to the reactants dimethyl ether and the aluminium atom[a]

structure	Method: B3LYP/6-311 + (2df,p) //B3LYP/6-31G(d,p)[b]	Method: BP86/6-311 + (2df,p) //B3LYP/6-31G(d,p)[c]
addition complex	−4.9(−4.1)	−9.1(−8.3)
di-ligand complex	−10.9	−13.3
TS1	25.8(20.7)	21.3(16.2)
C1-*cis*	21.6(17.0)	21.2(16.6)
C1-*trans*	21.4(17.0)	20.6(16.2)
TS2 (*cis*)	23.2(18.4)	21.9(17.1)
TS2 (*trans*)	25.7(21.2)	19.6(15.1)
C2-*cis*	−7.4(−10.2)	−10.5(−13.2)
C2-*trans*	−6.8(−9.7)	−9.9(−12.8)
TS2 (*cis–trans*)	−2.9(−6.1)	−6.3(−9.5)
TS3 (*cis–cis*)	−3.6(−7.0)	−6.8(−10.2)
TS3 (*trans–trans*)	−2.9(−6.5)	−6.3(−9.9)
TS3 (*cis–trans*p)	−4.3(−8.0)	−6.7(−10.4)
TS3 (*trans–trans*p)	−2.7(−6.6)	−5.4(−9.3)
TS3 (*cis–cis*p)	−4.8(−8.5)	−7.1(−10.8)
C3-*cis*p	−4.9(−8.7)	−7.4(−11.2)
C3-*trans*p	−5.4(−9.1)	−7.9(−11.6)
C3-*cis*	−4.2(−7.6)	−7.4(−10.8)
C3-*trans*	−4.4(−7.9)	−7.7(−11.2)
TS4	6.0(4.1)	0.1(−1.8)
C4-*cis*	−60.7(−62.6)	−61.7(−63.6)
C4-*trans*	−62.1(−63.9)	−63.3(−65.1)
TS4 (*cis–trans*)	−60.5(−62.7)	−61.2(−63.4)

[a] ZPE corrections, calculated at the B3LYP/6-31G(d,p) level, are included for the values in parentheses. [b] Energy (E_h) of reactants: Al −242.386 697, DME −155.084 672, total −397.471 369. [c] Energy (E_h) of reactants: Al −242.383 618, DME −155.077 005, total −397.460 623.

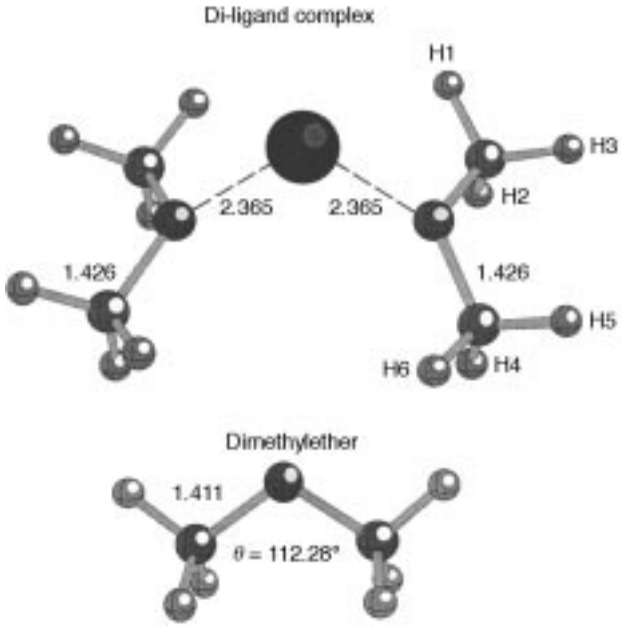

Fig. 1 Calculated (B3LYP/6-31G(d,p)) structures of the di-ligand complex and the free DME molecule

The energies of the addition complex and the di-ligand complex are 5–9 and 11–15 kcal mol^{-1} below that of the free reactants, respectively, depending on method used. This corresponds reasonably well with the experimentally determined gas phase value of the binding energy for the mono-ligand complex of 9.2 kcal mol^{-1}.[8]

C—H Insertion products. In the eight C—H insertion compounds the aluminium atom binds to the oxygen and one hydrogen atom (C1-*cis* and C1-*trans*); to the oxygen, one of the carbon and one of the hydrogen atoms (C2-*cis* and C2-*trans*); and to one of the carbon and one of the hydrogen atoms, in the last case forming both planar (C3-*cis*p, C3-*trans*p) and non-planar compounds (C3-*cis* and C3-*trans*), *cf.* Fig. 2, 3 and 4.

A transition state (TS1), in which a hydrogen has started to migrate to the aluminium atom, connects the addition complex with C1-*trans*. This transition state is 21.3–25.8 kcal mol^{-1} above the reactants giving a barrier for the insertion of the aluminium atom into the C–H bond of 30.4–32.9 kcal mol^{-1}, with the largest barrier observed at the B3LYP/6-31G(d,p) level and the lowest at the BP86 level (*cf.* Fig. 2 and Table 1). C1-*trans*, on the other hand, is a very high lying metastable minimum.

C1-*trans* is also connected with the more stable compound C2-*trans* through a second transition state (TS2-*trans*) in which the aluminium atom interacts also with one of the carbon atoms, *cf.* Fig. 2. TS2-*trans* is located 20–26 kcal mol^{-1} above the reactants in energy giving an energy barrier of a few kcal mol^{-1} for the passage to C2-*trans*, *cf.* Fig. 2. This compound together with the corresponding *cis* conformer (C2-*cis*) are the most stable C—H insertion products, 6.2–10.5 kcal mol^{-1} below the reactants in energy, with the *cis* compound slightly lower in energy of the two (Fig. 3 and Table 1). A transition state similar in shape to the C2 product struc-

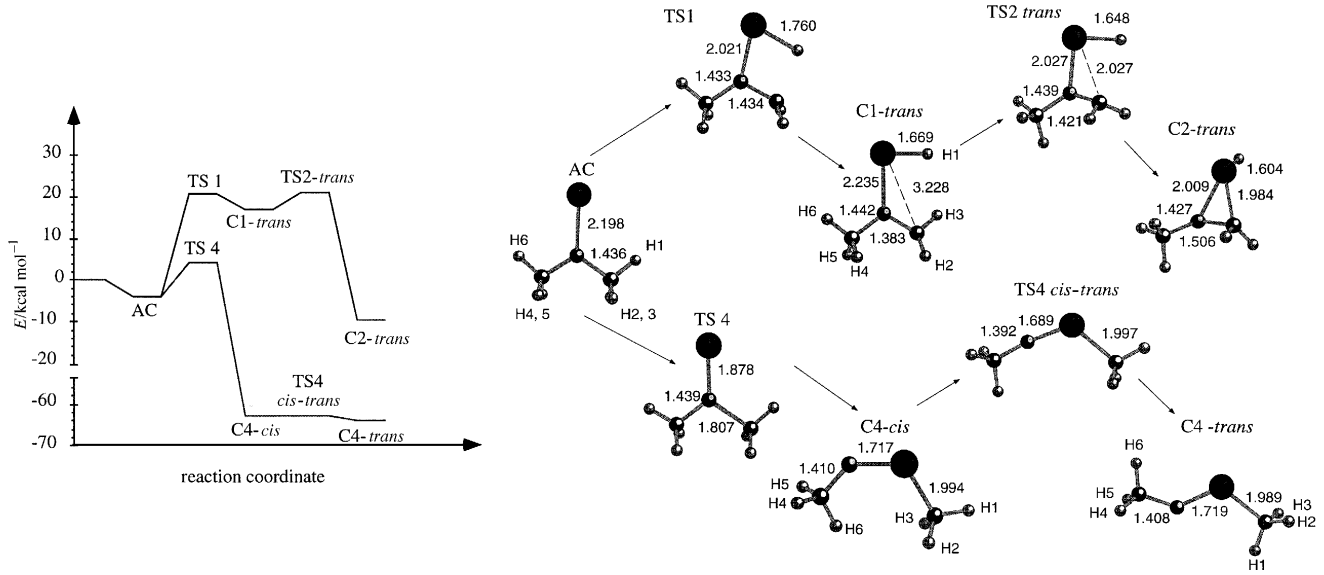

Fig. 2 Energy reaction profile for the C—H and C—O insertion reactions as well as geometrical structures of the C—H and C—O insertion products and transition states, optimized at the B3LYP/6-31G(d,p) level

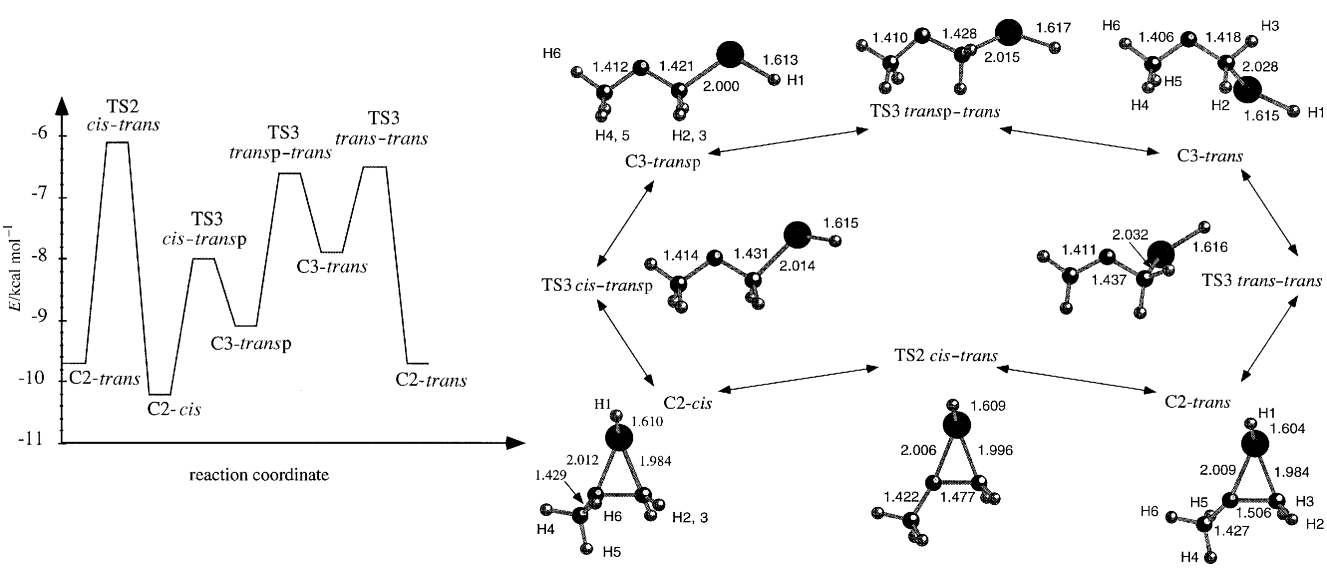

Fig. 3 Reaction profile for isomerization between different C—H insertion products and optimized structures of products and transition states

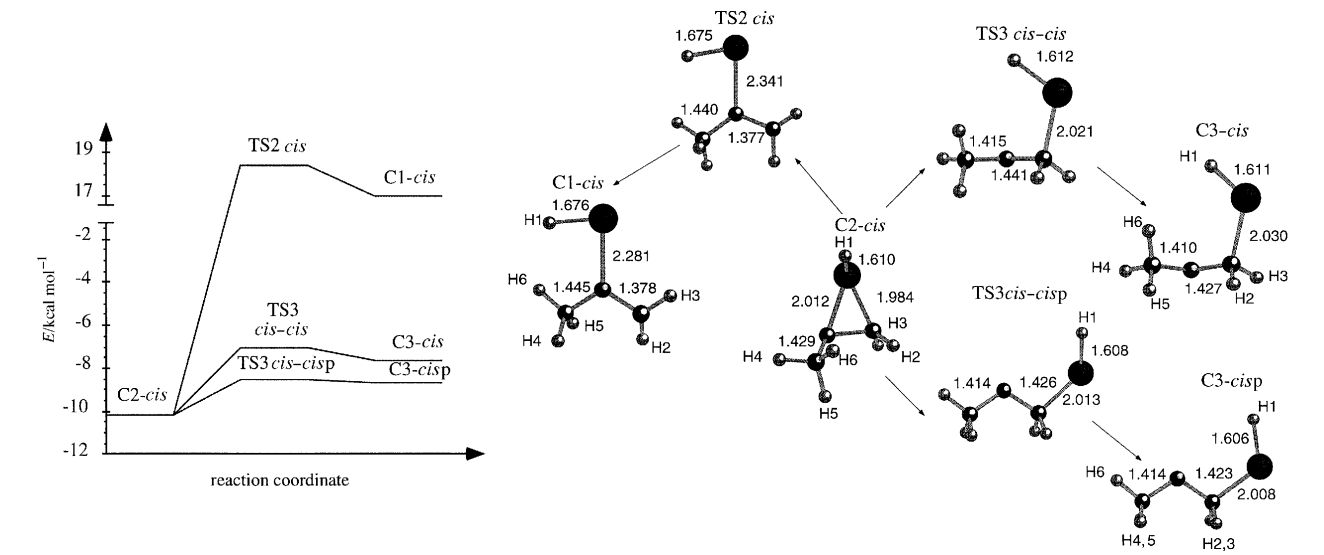

Fig. 4 Reaction profile for isomerization between different C—H insertion products and optimised structures of products and transition states

Table 2 Isotropic HFCC in gauss for possible products in the reaction between dimethyl ether and an aluminium atom.[a] Method: BP86/6-311 + G(2fd,p)//B3LYP/6-31G(d,p)

compound	Al	H1	H2	H3	H4	H5	H6
addition complex	−21.9	0.0	0.4	0.4	0.4	0.4	0.0
di-ligand complex	−22.6	0.0	0.6	0.1	0.6	0.1	0.1
C1-*cis*	1.3	0.2	−9.6	−13.2	2.7	3.6	−0.5
C1-*trans*	4.5	6.1	−9.2	−12.4	3.4	1.8	−0.3
C2-*cis*	306.5(II)	57.6(II)	3.3	−1.4	0.7	0.4	0.2
C2-*trans*	287.6	58.6	3.8	0.1	−0.2	−0.2	0.0
C3-*cis*	195.4	43.3	−0.5	−1.5	0.1	0.3	1.0
C3-*trans*	205.0	40.9	6.0	3.1	1.1	2.7	−0.1
C3-*cis*p	220.2	52.4	−1.9	−1.9	−0.3	−0.3	0.9
C3-*trans*p	253.1	50.9	1.9	1.9	0.1	0.1	0.3
C4-*cis*	333.9	−3.0	1.9	1.4	−0.7	−0.7	−0.4
C4-*trans*	269.8(IV)	5.0	−2.7	−2.3	−0.1	0.0	0.6

[a] The roman numbers correspond to the experimentally observed species (*cf.* Table 4).

Table 3 Isotropic HFCC (in G) for possible products in the reaction between dimethyl ether and an aluminium atom.[a] Method: B3LYP/6-311 + G(2fd,p)//B3LYP/6-31G(d,p)

compound	Al	H1	H2	H3	H4	H5	H6
addition complex	−15.8	0.0	0.1	0.1	0.1	0.1	0.0
di-ligand complex	−18.1	0.0	0.6	0.1	0.6	0.1	0.1
C1-*cis*	0.9	0.4	−10.8	−14.6	2.2	3.0	−0.4
C1-*trans*	0.5	3.9	−10.2	−14.2	2.9	1.5	−0.3
C2-*cis*	324.2(II)	66.0(II)	3.2	−1.6	0.7	0.5	0.2
C2-*trans*	304.2	67.3	4.0	−0.3	−0.1	−0.1	0.0
C3-*cis*	217.1	54.5	−1.1	−1.8	0.1	0.1	0.6
C3-*trans*	229.5	52.1	5.3	2.9	0.7	2.2	−0.1
C3-*cis*p	235.2	62.7	−1.9	−1.9	−0.3	−0.3	0.9
C3-*trans*p	271.1	60.9	1.8	1.8	0.1	0.1	0.4
C4-*cis*	346.5	−3.4	1.2	1.8	−0.4	−0.4	−0.4
C4-*trans*	285.5(IV)	5.2	−3.1	−2.6	0.0	0.1	0.3

[a] The roman numbers correspond to the experimentally observed species (*cf.* Table 4).

tures but with the aluminium, oxygen and the two carbon atoms in one plane (TS2-*cis*–*trans*) connects the *cis* and *trans* forms of C2 (*cf.* Fig. 3). The barrier corresponding to this *cis*–*trans* interconversion is 3.6–4.7 kcal mol^{-1}, with the largest barrier again obtained at the B3LYP/6-31G(d,p) level and the lowest at the BP86 level. The same trend was also observed for the low barrier between C1-*trans* and C2-*trans*, which vanishes at the BP86/6-311 + G(2df,p)//B3LYP/6-31(d,p) level (*cf.* Table 1 and Fig. 2).

The local minima where the aluminium atom binds solely to the transferred hydrogen and one of the carbons (compounds denoted C3) are reached from C2-*cis* and -*trans*. The planar *trans* compound, C3-*trans*p, is connected with C2-*cis* through an open chain transition state (TS3 *cis*–*trans*p) in which the Al—O bond is broken. C3-*trans* is reached from C2-*trans* through TS3 *trans*–*trans* in which again the Al—O bond is broken (*cf.* Fig. 3). The C2 and C3 structures are observed to be separated by small energy barriers of 2.6–4.7 kcal mol^{-1}.

Finally, two of the C3 compounds, C3-*trans*p and C3-*trans*, are connected through TS3 *trans*p–*trans* with an energy barrier varying between 2.5 and 3.0 kcal mol^{-1} depending on method (Fig. 3).

The remaining energy minima, C1-*cis*, C3-*cis* and C3-*cis*p can all be reached from C2-*cis* (*cf.* Fig. 4). Breaking the Al—C bond in C2-*cis*, C1-*cis* is reached through TS2-*cis* with an energy barrier of about 30 kcal mol^{-1}. Finally, breaking the Al—O bond C3-*cis* and C3-*cis*p are reached from C2-*cis* through two open chain transition states TS3 *cis*–*cis* and TS3 *cis*–*cis*p. The energy barriers are in the order of 2.6–4.7 kcal mol^{-1} with the barrier leading to the C3-*cis*p structure slightly lower (*cf.* Fig. 4).

The different C3 compounds are all found at 2.7–7.9 kcal mol^{-1} below the reactants, and hence lie a few kcal mol^{-1} above the two C2 compounds (*cf.* Table 1).

Table 4 Experimental isotropic HFCC (in G) for the reaction between dimethyl ether and an aluminium atom[a]

Species	Al	H1	H2	H3
I	357.5	—	—	—
II	294.7	58.9	—	—
III	318.6	—	—	—
IV	269.4	—	—	—

[a] The experimental values are from the work by Chenier *et al.*[10]

C—O Insertion products. Two C—O insertion products, one *cis* (C4-*cis*) and one *trans* (C4-*trans*), were located (*cf.* Fig. 2). The addition complex is connected to the *cis* form of the C—O insertion compounds (C4-*cis*), which is 56.5–61.7 kcal mol^{-1} below the reactants in energy, through a transition state (TS4) with an elongated O—C bond. TS4 is located 0.1–6.4 kcal mol^{-1} above the reactants in energy giving a barrier for the C—O insertion ranging from 9.2 to 13.5 kcal mol^{-1} depending on the method. Just as for the Al insertion into the C—H bond, the B3LYP/6-31(d,p) method predicts the highest and BP86 the lowest energy barrier. C4-*cis* is further connected to the most stable stationary point encountered at the PES, the *trans* C—O insertion product (C4-*trans*), through a transition state with a close to linear C—O—Al fragment (TS4 *cis*–*trans*), *cf.* Fig. 2. C4-*trans* is 58.1–63.3 kcal mol^{-1} more stable than the reactants, depending on method. The small barrier separating the *cis* from the *trans* conformers is calculated to be between 0.2 and 0.8 kcal mol^{-1}.

Zero point vibrational energy corrections. Zero point vibrational energy corrections (ZPE) were calculated for all stationary points at the B3LYP/6-31(d,p) level. The corrections stabilize all transition states and product structures by 1.8 to 5.1 kcal mol^{-1} and destabilize the addition complex by *ca.* 0.8 kcal mol^{-1}. All energy barriers are thus lowered somewhat, from a few tenths of a kcal mol^{-1} up to 2.7 kcal mol^{-1}, when

the ZPE corrections are included. The one exception is the barrier separating the addition complex from C1-*trans* for which a somewhat larger lowering of *ca.* 6 kcal mol^{-1} is observed when the correction is included. Owing to the small basis set superposition errors observed in a previous study of the Al + propene system, using similar methods as those employed here,[37] no such corrections were calculated in the present paper.

Hyperfine coupling constants

The isotropic HFCC are reported for the hydrogens and the aluminium atom of the addition complex, the di-ligand complex and the insertion products from single point calculations employing the larger basis set. The calculated and experimentally observed couplings are presented in Tables 2–4.

Very good agreement with the experimental spectrum (II) is observed at the BP86 level for the *cis* structure of the most stable C—H insertion product (C2-*cis*) [*cf.* Fig. 3 and Tables 2 and 4]. The deviations between calculated and experimental values for the aluminium atom and the migrated proton, H1, are less than 4.5%. Also at the B3LYP level good agreement between experimental and calculated values is observed, with deviations between calculated and experimental values of less than 10.5% for the Al HFCC and less than 12.5% for the proton HFCC. The agreement between experimental and calculated values is even somewhat better for the *trans* compound. However, the assignment that the *cis* conformer of C2 corresponds to the observed C—H insertion product is supported by the calculated energetic stability of the products, with C2-*cis* 0.5–3.8 kcal mol^{-1} more stable compared to the other C—H insertion products. The calculated HFCC for the remaining protons, H2–H6, for both the *cis* and *trans* conformers of compound **2** are less than 4.5 G irrespective of method used, which suggests why no β proton HFCCs were resolved in the experimental EPR spectra.

The experimentally observed sextet with a splitting of 269.4 G (IV) was previously assigned to either an addition or a di-ligand complex.[10] Considering the extremely poor agreement with the calculated HFCC for the complexes, *cf.* Tables 2–4, we suggest a reassignment of the observed splitting to one of the C—O insertion products. The observed experimental value agrees excellently with the calculated Al HFCC for the most stable C—O insertion product, C4-*trans*, at the BP86/6-311 + G(2df,p)//B3LYP/6-31G(d,p) level. The calculated value deviates 0.2 and 6% from the experimental value at the BP86 and B3LYP levels, respectively. The maximum calculated proton HFCC for the C—O insertion products was again very small; 5.2 G (*cf.* Tables 2 and 3 and Fig. 2). The calculated energetic stability of the products supports the assignment of C4-*trans* to one of the experimentally observed species.

The assignment of the observed proton and Al HFCC for C2-*cis* and C4-*trans* using the HFCC calculated at the BP86/6-311 + G(2df,p)//B3LYP/6-31G(d,p) level and, shown in parentheses, at the B3LYP/6-311 + G(2df,p)//B3LYP/6-31G(d,p) level, are as follows (*cf.* Fig. 2 and 3 and Tables 2–4). *cis* Structure of the C—H insertion product (C2-*cis*): Al: experimental value 294.7 G, computed 306.5 G (324.2 G); H1: experimental value 58.9 G, computed 57.6 G (66.0 G); *trans* structure of the C—O insertion product (C4-*trans*): Al: experimental value 269.4 G, computed 269.8 G (285.5 G).

The two remaining sextets observed experimentally, with splittings of 318.6 and 357.5 G can not be uniquely assigned to any of the stationary points found. From the very poor agreement between the calculated values for the two addition complexes and the two experimentally observed splittings we conclude that neither of the latter corresponds to an addition or di-ligand complex. Both the calculated relative energies and the calculated HFCC clearly exclude the possibility that C1-*cis* and -*trans* have been observed in the experiment. Neither of the remaining C2 or C3 compounds could clearly be identified with the two unassigned species because of their large calculated proton HFCC.

Discussion and Summary

Stationary points have been located for the reaction between aluminium and dimethyl ether at the B3LYP and BP86 levels. Both methods give qualitatively the same results although the barriers differ slightly depending on method. In general the relative energies are predicted to be lowest at the BP86/6-311 + G(2df,p)//B3LYP/6-31G(d,p) level with the one exception of the di-ligand complex which is observed to be lowest in energy at the B3LYP/6-31G(d,p) level.

Possible reaction paths for both the Al C—H and C—O insertion reactions are outlined. Based on the results in this theoretical investigation, the Al atom breaks a C—H bond in the methyl group to eventually form a (H)Al product in which the aluminium atom binds to both the carbon and oxygen atoms. The reaction path involves an Al—O addition complex, a first transition state leading to a structure in which one hydrogen has migrated to the Al atom, whereafter a more stable C—H insertion structure is reached through a second transition state. When the C—O insertion product is formed, the Al atom instead breaks one of the C—O bonds to form the insertion product. This second reaction path involves, except for the addition complex, a first transition state leading to a *cis* form of an open chain C—O insertion structure, whereafter the more stable *trans* form is reached through a second transition state. The ZPE corrected barriers for the C—H and C—O insertion reactions were calculated to be 24.5–27.0 and 6.5–10.8 kcal mol^{-1}, respectively, depending on method. Both barriers were calculated to be lowest at the BP86/6-311 + G(2df,p)//B3LYP/6-31G(d,p) level and highest at the B3LYP/6-31G(d,p) level.

The hyperfine coupling constants for the possible products have been determined using the 6-311 + G(2df,p) basis in conjunction with the B3LYP and BP86 functionals. There is good agreement between the computed and experimental HFCC for two of the products found, namely the *cis* structure of the most stable C—H insertion product and the *trans*-C—O insertion product. This supports the two suggested reaction paths towards a $HAlCH_2CH_2CH_3O$ complex as one of the final products and the C—O insertion product CH_3AlOCH_3 as a second. Best overall agreement between calculated and experimental HFCC is obtained at the BP86/6-311 + G(2df,p) //B3LYP/6-31G(d,p) level of theory in which the calculated values differ at most 4.5% and at average 2.2% from the experimental values. Two experimentally observed sextets with splittings of 318.6 and 357.5 G were not possible to uniquely assign to any of the stationary points found. None of the points located in the present paper was clearly possible to identify as the carrier of the two experimentally observed sextets, either due to calculated relative stability and energy barriers and/or due to poor agreement between calculated and experimental HFCC values.

The unassigned sextets might correspond to complex formation between DME and some of the found product structures.

The Swedish Natural Sciences Research Council (NFR) is gratefully acknowledged for financial support. Grants of computer time on the IBM SP at the Center for Parallel Computers (PDC) in Stockholm and the Cray C90 of the Swedish

Supercomputer Center (NSC) in Linköping are gratefully acknowledged.

References

1 P. H. Kasai and P. McLeod Jr., *J. Am. Chem. Soc.*, 1975, **97**, 5609.
2 P. H. Kasai, *J. Am. Chem. Soc.*, 1982, **104**, 1165.
3 J. A. Howard, B. Mile, J. S. Tse and H. Morris, *J. Chem. Soc., Faraday Trans.*, 1987, **83**, 3701.
4 P. H. Kasai, P. McLeod Jr. and T. Wafanabe, *J. Am. Chem. Soc.*, 1977, **99**, 3521.
5 J. H. B. Chenier, J. A. Howard, J. S. Tse and B. Mile, *J. Am. Chem. Soc.*, 1985, **107**, 7290.
6 P. S. Skell and L. R. Wolf, *J. Am. Chem. Soc.*, 1972, **94**, 7919.
7 P. H. Kasai and P. McLeod Jr., *J. Am. Chem. Soc.*, 1979, **101**, 5860.
8 J. M. Parnis, S. A. Mitchell, D. M. Rayner and P. A. Hackett, *J. Phys. Chem.*, 1988, **92**, 3869.
9 J. A. Howard, H. A. Joly and B. Mile, *J. Chem. Soc., Faraday Trans.*, 1990, **86**, 219.
10 J. H. Chenier, J. A. Howard, H. A. Joly, M. LeDuc and B. Mile, *J. Chem. Soc., Faraday Trans.*, 1990, **86**, 3321.
11 S. Sakai, *J. Phys. Chem.*, 1993, **97**, 8917.
12 S. J. Silva and J. D. Head, *J. Am. Chem. Soc.*, 1992, **114**, 6479.
13 C. J. Cramer, *J. Mol. Struct. (THEOCHEM)*, 1991, **235**, 243.
14 M. Trenary, M. E. Casida, B. R. Brooks and H. F. Schaefer III, *J. Am. Chem. Soc.*, 1979, **101**, 1638.
15 J. Q. Su, Y. Xie and H. F. Schaefer III, *Chem. Phys. Lett.*, 1990, **170**, 301.
16 D. J. Fox, D. Ray, P. C. Rubesin and H. F. Schaefer III, *J. Chem. Phys.*, 1980, **73**, 3246.
17 M. J. Frisch, G. W. Trucks, H. B. Schlegel, P. M. W. Gill, B. G. Johnson, M. W. Wong, J. B. Foresman, M. A. Robb, M. Head-Gordon, E. S. Replogle, R. Gomperts, J. L. Andres, K. Raghavachari, J. S. Binkley, C. Gonzalez, R. L. Martin, D. J. Fox, D. J. Defrees, J. Baker, J. P. Stewart and J. A. Pople, Gaussian 92/DFT, Revision G.3, Gaussian, Inc., Pittsburgh PA, 1993.
18 M. J. Frisch, G. W. Trucks, H. B. Schlegel, P. M. W. Gill, B. G. Johnson, M. A. Robb, J. R. Cheeseman, T. Keith, G. A. Petersson, J. A. Montgomery, K. Raghavachari, M. A. Al-Laham, V. G. Zakrzewski, J. V. Ortiz, J. B. Foresman, J. Cioslowski, B. B. Stefanov, A. Nanayakkara, M. Challacombe, C. Y. Peng, P. Y. Ayala, W. Chen, M. W. Wong, J. L. Andres, E. S. Replogle, R. Gomperts, R. L. Martin, D. J. Fox, J. S. Binkley, D. J. Defrees, J. Baker, J. P. Stewart, M. Head-Gordon, C. Gonzalez and J. A. Pople, Gaussian 94, Revision B.2, Gaussian, Inc., Pittsburgh PA, 1995.
19 A. D. Becke, *J. Chem. Phys.*, 1993, **98**, 5648.
20 J. C. Slater, *Quantum Theory of Molecular and Solids vol. 4: The Self-Consistent Field for Molecular and Solids*, McGraw-Hill, New York, 1974.
21 V. Fock, *Z. Phys.*, 1930, **61**, 126.
22 A. D. Becke, *Phys. Rev. A*, 1988, **38**, 3098.
23 L. Wilk, S. H. Vosko and M. Nusair, *Can. J. Phys.*, 1980, **58**, 1200.
24 C. Lee, W. Yang and R. G. Parr, *Phys. Rev. B*, 1988, **37**, 785.
25 P. C. Hariharan and J. A. Pople, *Theor. Chim. Acta*, 1973, **28**, 213.
26 M. M. Francl, W. J. Petro, W. J. Hehre, J. S. Binkley, M. S. Gordon, D. J. DeFrees and J. A. Pople, *J. Chem. Phys.*, 1982, **77**, 3654.
27 R. Krishnan, J. S. Binkley, R. Seeger and J. A. Pople, *J. Chem. Phys.*, 1980, **72**, 650.
28 A. D. McLean and G. S. Chandler, *J. Chem. Phys.*, 1980, **72**, 5639.
29 T. Clark, J. Chandrasekhar, G. W. Spitznagel and P. von R. Schleyer, *J. Comput. Chem.*, 1983, **4**, 294.
30 P. M. W. Gill, G. B. Johnson, J. A. Pople and M. J. Frisch, *Chem. Phys. Lett.*, 1992, **197**, 499.
31 M. J. Frisch, J. A. Pople, J. S. Binkley and P. von R. Schleyer, *J. Chem. Phys.*, 1984, **80**, 3265.
32 J. P. Perdew, *Phys. Rev. B*, 1986, **33**, 8822.
33 E. Fermi, *Z. Phys.*, 1930, **60**, 320.
34 E. Fermi and E. Segre, *Z. Phys.*, 1933, **82**, 729.
35 C. Gonzalez and H. B. Schlegel, *J. Chem. Phys.*, 1989, **90**, 2154.
36 C. Gonzalez and H. B. Schlegel, *J. Phys. Chem.*, 1990, **94**, 5523.
37 T. Fängström, L. A. Eriksson and S. Lunell, *J. Phys. Chem. A*, 1997, **101**, 4814.

Paper 7/06667H; *Received* 15*th September*, 1997